

24. C. E. Forest, P. H. Stone, A. P. Sokolov, M. R. Allen, M. D. Webster, *Science* **295**, 113 (2001).
25. Transient temperature change in 2100 is not, in general, equilibrium change. The inertia of the climate system is such that climate change will continue long after greenhouse gas concentrations are stabilized or emissions eliminated. Some outcomes that avoid exceeding a DAI threshold until 2100 will exceed that threshold in the next century. Therefore, the time horizon of analysis will affect the potential for DAI. However, what is "dangerous" is itself a function of adaptive capacity, not a static quantity, dependent on social and economic development. So, the very threshold for any percentile X , $DAI[X\%]$, can itself change with time and social conditions.
26. In the DICE model, carbon taxes serve as a proxy for general climate policy controls. Thus, we do not present carbon tax data as a preferred method for mitigation or a required method to produce our results. Instead, these results should be seen as a method to provide insights into coupled model behavior, using the carbon tax in DICE as a measure of the magnitude of climate policy controls.
27. Results such as this are extremely sensitive to the discount rate. For example, the increase in the climate damage function indicated above that produces a ~45% reduction in the probability of $DAI[50\%]$ with a 0% PRTP produces a reduction of only ~10% and an order of magnitude lower "optimal" carbon tax when we used a 3% PRTP, the value employed by the original DICE model. We chose to use a 0% PRTP for Fig. 3 exactly for this reason—that using a high discount rate masks the variation in model results because of changes in parameters other than the discount rate, and observing variation in model results due to other parameters is central to our analysis.
28. We consider three of these sources of uncertainty in the three parameters we varied, but there are other important sources of uncertainty. The DICE model does not consider adaptation, as opposed to mitigation, which theoretically would shift the probability distribution for DAI to higher temperature levels. A highly adaptive society would be less likely to experience dangerous impacts, although this would not be as likely to apply to the first reason for concern, damages to natural systems. The DICE model also only considers mitigation policies for CO_2 . It does not account for "knock-on" impacts of CO_2 reductions on emissions of other atmospheric substances, and it specifies a fixed path for non- CO_2 greenhouse gases. Alternative emissions pathways for non- CO_2 gases and for other anthropogenic radiative forcing agents such as aerosols would also affect the potential for DAI.
29. R. J. Lempert, M. E. Schlesinger, *Clim. Change* **45**, 387 (2000).
30. T. Wigley, *Clim. Change*, in press.
31. C. Azar, H. Rodhe, *Science* **276**, 1818 (1997).
32. B. C. O'Neill, M. Oppenheimer, *Science* **296**, 1971 (2002).
33. We thank T. Wigley, K. Kuntz-Duriseti, J. Bushinsky, and M. Hayes for constructive comments on previous drafts. Supported by the Global Change Education Program of the Department of Energy and the Interdisciplinary Graduate Program in Environment and Resources at Stanford University (M.D.M.) and by the Winslow Foundation (S.H.S.).

Supporting Online Material

www.sciencemag.org/cgi/content/full/304/5670/571/DC1

Materials and Methods

Fig. S1

References and Notes

1 December 2003; accepted 19 March 2004

Timing, Duration, and Transitions of the Last Interglacial Asian Monsoon

Daoxian Yuan,¹ Hai Cheng,² R. Lawrence Edwards,^{2*} Carolyn A. Dykoski,² Megan J. Kelly,² Meiliang Zhang,¹ Jiaming Qing,¹ Yushi Lin,¹ Yongjin Wang,³ Jianguyin Wu,³ Jeffery A. Dorale,⁴ Zhisheng An,⁵ Yanjun Cai⁵

Thorium-230 ages and oxygen isotope ratios of stalagmites from Dongge Cave, China, characterize the Asian Monsoon and low-latitude precipitation over the past 160,000 years. Numerous abrupt changes in $^{18}O/^{16}O$ values result from changes in tropical and subtropical precipitation driven by insolation and millennial-scale circulation shifts. The Last Interglacial Monsoon lasted 9.7 ± 1.1 thousand years, beginning with an abrupt (less than 200 years) drop in $^{18}O/^{16}O$ values 129.3 ± 0.9 thousand years ago and ending with an abrupt (less than 300 years) rise in $^{18}O/^{16}O$ values 119.6 ± 0.6 thousand years ago. The start coincides with insolation rise and measures of full interglacial conditions, indicating that insolation triggered the final rise to full interglacial conditions.

The characterization of past climate is often limited by the temporal resolution, geographic coverage, age precision and accuracy, and length and continuity of available records. Among the most robust are ice core records (1, 2), which characterize, among other measures of climate, the oxygen isotopic composition of precipitation.

Although many such records are benchmarks, they are limited to high-latitude or high-elevation sites, which record the oxygen isotopic composition of the last fraction of atmospheric moisture remaining after transit from moisture source regions. Cave calcite also contains information about the isotopic composition of meteoric precipitation, is widespread, and can be dated with ^{230}Th methods. Thus, caves may yield well-dated, low-latitude, low-elevation records that characterize atmospheric moisture earlier in its transit from source regions. We report here on such a record of Asian Monsoon precipitation, which covers most times since the penultimate glacial period, about 160 thousand years ago (ka).

We have previously reported a cave oxygen isotope record of the East Asian Monsoon (3) from Hulu Cave, China [$32^{\circ}30'N$,

$119^{\circ}10'E$; elevation 100 m; cave temperature $15.7^{\circ}C$; mean annual precipitation $\delta^{18}O_{VSMOW} = -8.4$ per mil (‰) (VSMOW, Vienna standard mean ocean water); and mean annual precipitation 1036 mm] (table S1), covering the last glacial period [75 ka to 10 thousand years (ky) before the present]. We now report similar data from Dongge Cave, China, 1200 km WSW of Hulu Cave, a site affected by the Asian Monsoon. The Dongge record more than doubles the time range covered in the Hulu record and overlaps the Hulu record for ~35 ky, allowing comparison between sites. Highlights include the timing and rapidity of the onset (4) and end of the Last Interglacial Asian Monsoon and the degree of Last Interglacial Monsoon variability.

Dongge Cave is 18 km SE of Libo, Guizhou Province ($25^{\circ}17'N$, $108^{\circ}5'E$), at an elevation of 680 m. The cave temperature ($15.6^{\circ}C$), mean annual $\delta^{18}O$ of precipitation (-8.3%), and seasonal changes in precipitation and $\delta^{18}O$ of precipitation are similar to those at Hulu, with mean annual precipitation being higher (1753 mm) (table S1). Stalagmites D3 and D4 were collected ~100 m below the surface, 300 and 500 m from the entrance, in the 1100-m-long main passageway. D3 is 210 cm and D4 is 304 cm long, with the diameters of each varying between 12 and 20 cm. Stalagmites were halved vertically and drilled along growth axes to produce subsamples for oxygen isotope analysis (5) and ^{230}Th dating by thermal ionization (6, 7) and inductively coupled plasma mass spectroscopy (8). Sixty-six ^{230}Th dates from D3 and D4 (table S2) and 10 dates from Hulu Cave stalagmite H82 (table S3), all in stratigraphic order, have 2σ analytical errors of ± 80 years at 10 ky and ± 1 ky at 120 ky. Six hundred and forty $\delta^{18}O$ measurements have spatial resolution corresponding to 20 years to 2 ky for different portions of D3 and D4

¹Karst Dynamics Laboratory, Ministry of Land and Resources, 40 Qixing Road, Guilin 541004, China. ²Department of Geology and Geophysics, University of Minnesota, Twin Cities, MN 55455, USA. ³College of Geography Science, Nanjing Normal University, Nanjing 210097, China. ⁴Department of Geoscience, University of Iowa, Iowa City, IA 52242, USA. ⁵State Key Lab of Loess and Quaternary Geology, Institute of Earth Environment, Chinese Academy of Sciences, Xi'an 710075, China.

*To whom correspondence should be addressed. E-mail: edwar001@umn.edu

(Dongge Cave, table S4), and 830 $\delta^{18}\text{O}$ measurements on H82 have average spatial resolution corresponding to 7 years (Hulu Cave, table S5).

A key issue is whether stalagmite $\delta^{18}\text{O}$ values (Figs. 1 and 2) can be interpreted solely in terms of the $\delta^{18}\text{O}$ of precipitation and cave temperature. The general replication (3) of $\delta^{18}\text{O}$ values for 35 ky of contemporaneous growth, for D3 and D4 (Fig. 2), argues

that the $\delta^{18}\text{O}$ values are not strongly affected by water/rock interactions or kinetic fractionation (9, 10). Although we have not yet identified young calcite from Hulu, D4's youngest calcite (Fig. 2) was deposited in isotopic equilibrium, because its $\delta^{18}\text{O}$ value, the mean annual $\delta^{18}\text{O}$ of modern meteoric precipitation, and mean annual temperature (table S1) satisfy the equilibrium calcite/water fractionation equation (11). For times of contempo-

aneous deposition of D4 and the Hulu Cave stalagmites (~35 ky), the caves' records replicate remarkably well (Figs. 1 and 2), indicating not only that the calcite $\delta^{18}\text{O}$ can largely be interpreted in terms of the $\delta^{18}\text{O}$ of meteoric precipitation and cave temperature, but also that the two sites have a similar history of meteoric $\delta^{18}\text{O}$ and cave temperature. Because Dongge is 1200 km from Hulu, this generalizes the Hulu results to areas well to the southwest. Indeed, the broad trends in the Dongge/Hulu data have similarities with Northern Hemisphere tropical and subtropical records at least as far west as the Middle East (12, 13) and probably as far away as northern South America (14).

An important characteristic of the Hulu/Dongge record (Fig. 2) is the large amplitude of the oxygen isotope ratio: 4.7‰. Because the change in the calcite/water fractionation of oxygen isotopes with temperature is small [-0.23‰ per °C (11)], the amplitude must result largely from changes in the $\delta^{18}\text{O}$ of meteoric precipitation. A second important observation is the general anticorrelation between $\delta^{18}\text{O}$ values at Hulu Cave and in Greenland ice during the last glacial period and the last deglaciation (Figs. 1 and 2) (3), a relation that has now been observed at a number of northern low-latitude sites [Israel (12) and Venezuela (14), in addition to Hulu (3) and Dongge Caves].

Interpretations of changes in precipitation $\delta^{18}\text{O}$ have focused on (i) the correlation between mean annual temperature and $\delta^{18}\text{O}$ of modern meteoric precipitation [for temperatures <10°C (15)] and (ii) the anticorrelation between rainfall amount and precipitation $\delta^{18}\text{O}$ [the "amount effect" (15)]. However, modern precipitation $\delta^{18}\text{O}$ trends basically result from the progressive removal of water vapor from air masses as they move from moisture source regions, resulting in decreasing water vapor and precipitation $\delta^{18}\text{O}$, which explains the first-order observation of lower precipitation $\delta^{18}\text{O}$ values at higher latitudes. Precipitation $\delta^{18}\text{O}$ at Hulu/Dongge is therefore largely a measure of the fraction of water vapor removed from air masses between the tropical Indo-Pacific and southeastern China. To first order, this process can be modeled assuming Rayleigh fractionation (15). Although more sophisticated models may ultimately be useful, any model for which meteoric $\delta^{18}\text{O}$ decreases with the removal of water vapor will lead us, at least qualitatively, to the conclusions below. Using the standard Rayleigh equation (16), the percentage of water vapor lost before reaching Hulu/Dongge is 63% (16) during the mid-Holocene and Last Interglacial Period, 59% (16) today, and 52% (16) during glacial periods [about 16 ka (Heinrich Event I) and immediately before and after the Last Interglacial Period], indicating that rainfall

Fig. 1. Comparison between the $\delta^{18}\text{O}$ time series of Dongge and Hulu Caves during the last deglaciation and early Holocene, with error bars indicating ^{230}Th ages and errors. Because the sites are separated by 1200 km, the records need not replicate. The striking similarity indicates not only that kinetic factors and water/rock interactions are not likely to have affected the cave $\delta^{18}\text{O}$ values, but also that the history of the oxygen isotopic composition of precipitation and temperature at the two sites is similar. B.P., before the present.

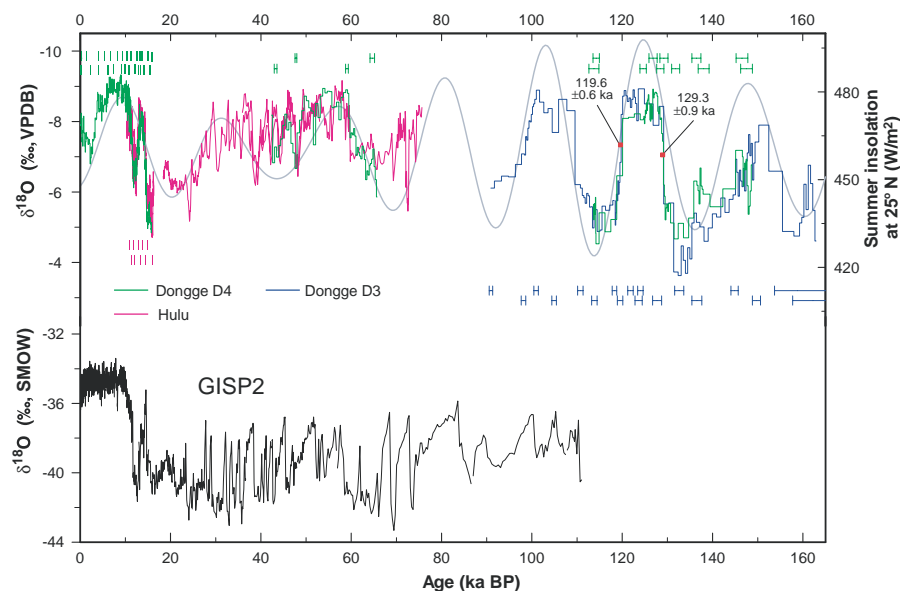
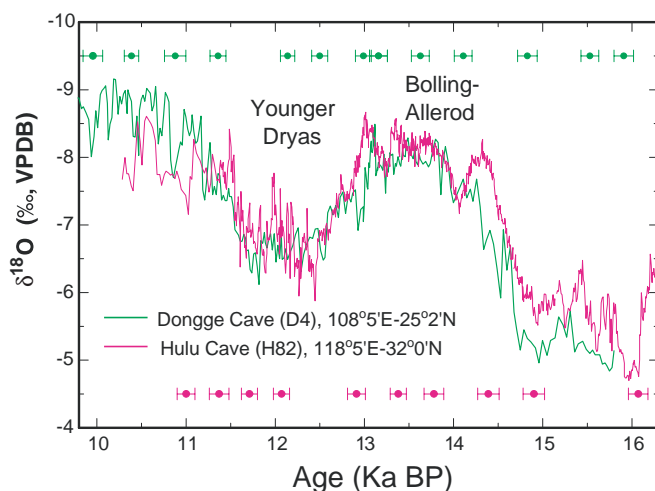


Fig. 2. (Top) $\delta^{18}\text{O}$ values of Dongge Cave stalagmites D3 (blue) and D4 (green) and Hulu Cave stalagmites {purple, including H82 [this study and (3)], MSD (3), and MSL (3)}. Dongge and Hulu Cave ^{230}Th ages and 2σ errors are color-coded by stalagmite (errors for dates <20 ka are equal to or less than the error bars). Summer insolation (integrated over June, July, and August) at 25°N is shown in gray (24). (Bottom) $\delta^{18}\text{O}$ values of Greenland ice (2). The $\delta^{18}\text{O}$ scale in the top section increases downward, whereas that of the bottom section increases upward. The Asian Monsoon is characterized throughout this interval by large abrupt (several years to a few centuries) shifts in $\delta^{18}\text{O}$, which anticorrelate with millennial-scale events as observed in Greenland and with insolation. The changes in stalagmite $\delta^{18}\text{O}$ likely reflect changes in the amount of precipitation between atmospheric moisture sources and cave localities, with decreases in $\delta^{18}\text{O}$ (up in top section) corresponding to increases in precipitation integrated from source to cave site.

integrated between tropical sources and southeast China was lower during glacial than interglacial times, perhaps related to lower relative humidity.

To estimate absolute amounts of rainfall integrated from sources to southeast China, we must make assumptions about absolute humidity in tropical source regions. Even assuming a glacial relative humidity as high as today's and only a modest tropical temperature depression (2.5°C), we calculate an absolute tropical glacial vapor pressure that is 85% of today's and 79% of mid-Holocene/Last Interglacial values (at a mid-Holocene temperature 1°C greater than today and constant relative humidity). Coupled with the Rayleigh calculations, the amount of precipitation integrated between tropical sources and southeast China is today ~87% of mid-Holocene/Last Interglacial values and ~65% of mid-Holocene/Last Interglacial values at glacial times corresponding to the heaviest Hulu/Dongge calcite $\delta^{18}\text{O}$ values, indicating that this region was significantly drier during glacial times. This phenomenon may be applicable to broad areas of the northern tropics and subtropics, because precipitation $\delta^{18}\text{O}$ records from Israel (12) and Venezuela (14) have the same general character as the Hulu/Dongge record (high $\delta^{18}\text{O}$ during glacial times), and Amazon discharge has been estimated to have been diminished by 40% or more during the Younger Dryas (17). Thus, the Hulu/Dongge record indicates major and abrupt changes in tropical and subtropical precipitation, which correlate with temperature in the North Atlantic region as recorded in Greenland ice.

Whatever the ultimate causes of the observed changes, the inferred moisture differences may play an important role in amplifying climatic change through feedbacks tied to water vapor's greenhouse properties. Because atmospheric general circulation modeling of glacial precipitation does not recover low-latitude $\delta^{18}\text{O}$ values as high (18, 19) as those observed here and elsewhere (12), it is plausible that this feedback is not fully captured in these models.

The timing of the Last Interglacial Period's onset [Termination II; see (4) and references therein], duration (6, 20–23), and ending have been the source of extensive research and controversy. The low $\delta^{18}\text{O}$ excursion associated with the Last Interglacial Asian Monsoon (Figs. 2 and 3) is characterized by (i) a large abrupt decrease in $\delta^{18}\text{O}$ of about 3‰ (Monsoon Termination II), which took place 129.3 ± 0.9 ka; (ii) $\delta^{18}\text{O}$ values varying within a range of ~1‰ for the ensuing 9.7 ± 1.1 ky; and (iii) a large and abrupt increase in $\delta^{18}\text{O}$ of about 3‰ 119.6 ± 0.6 ka. Based on constant growth rates, the transitions took place extremely rapidly: most of Monsoon Termination II in <200 years and

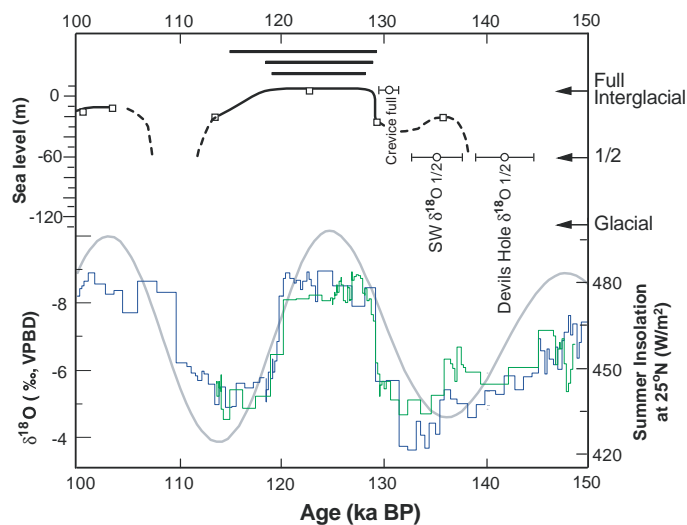
most of the transition at the end of the Last Interglacial in <300 years. Monsoon Termination II is similar in rapidity, magnitude, and relation to insolation to the transition into the Bølling-Allerød during Termination I (Fig. 1) (3). Thus, the rapidity of changes that characterizes the last glacial period also pertains to the glacial/interglacial transitions.

The Last Interglacial “square wave” is centered under the 25°N summer insolation peak (24). Monsoon Termination II takes place after a significant insolation rise, and the transition at the end of the Last Interglacial takes place after a significant insolation decrease, indicating that the low Last Interglacial Monsoon $\delta^{18}\text{O}$ values result from Northern Hemisphere insolation changes (25). Indeed, the low-frequency component of the whole Hulu/Dongge record (Fig. 3) correlates with insolation, indicating that insolation is important in controlling monsoon intensity as predicted (25). At higher frequency, the correlation between millennial-scale events in Greenland and southeast China indicates that Asian Monsoon changes are an integral part of millennial-scale reorganization of ocean/atmosphere circulation patterns (3). Although the timing of the Last Interglacial Monsoon is consistent with insolation forcing, the abruptness of the transitions indicates that the detailed mechanism likely includes threshold effects. Although smaller in range than that of the last glacial period,

the $\delta^{18}\text{O}$ range of the Last Interglacial Period (~1‰) is still significant, amounting to about half the amplitude of typical last glacial period monsoon interstadial events (Fig. 2) (3). This supports indications of Last Interglacial Monsoon variability from loess deposits (26) and the idea that, in addition to well-documented examples of glacial climate instability, interglacial climate is also characterized by substantial variability.

Monsoon Termination I (the transition into the Bølling-Allerød) and Monsoon Termination II are each characterized by an abrupt lowering of $\delta^{18}\text{O}$ in less than 200 years (Fig. 2). Both shifts occur after significant rises in summer insolation but before insolation peaks. The clearest difference is Termination I's prominent high $\delta^{18}\text{O}$ excursion during the Younger Dryas, a feature not observed in Monsoon Termination II, indicating that Younger Dryas-type events are not a general feature of terminations. Another difference is the fact that $\delta^{18}\text{O}$ trends toward lower values for several millennia after Termination I, whereas $\delta^{18}\text{O}$ values in the millennia immediately after Termination II do not follow a clear trend. Both differences could be related to ice volume, because sea level during and after Monsoon Termination II (27–29) may have been higher than during Termination I (30). If so, the cause of the Younger Dryas is likely to be ice sheet-related, and the intensity of the monsoon is affected by ice sheet volume.

Fig. 3. (Bottom) An enlargement of the portion of the Dongge $\delta^{18}\text{O}$ record around the Last Interglacial Period versus time. The gray curve is the summer (June, July, and August) insolation curve at 25°N (24). **(Top)** Portions of the direct sea level record [after (34)] and other directly dated measures of climate change. Error bars depict the ages of the half-height (1/2) of Devils Hole Termination II (20), the half-height of the marine oxygen isotope Termination II (29), and the first full interglacial $\delta^{18}\text{O}$ values at Crevice Cave, MO (36). The three black horizontal bars centered at ~125 ky indicate the duration of the Last Interglacial sea level high stand from Bahamian corals [upper bar (27)], Australian corals [middle bar (22)], and direct dating of the marine oxygen isotope record [lower bar (35)]. The timing of Monsoon Termination II coincides within error with insolation rise, the final rise of sea level (34), the final rise of Crevice Cave $\delta^{18}\text{O}$ (35), and the final rise of Soreq Cave $\delta^{18}\text{O}$ [not depicted (12)] to full interglacial values. Thus, Monsoon Termination II appears to mark the final insolation-forced rise to full Last Interglacial conditions. However, a number of events not directly caused by insolation change preceded Monsoon Termination II by thousands of years [Devils Hole Termination II (20), marine oxygen isotope Termination II (29), a significant fraction of the sea level rise toward interglacial values (27, 28), Antarctic temperature rise (not depicted) (4, 32, 33), and atmospheric CO_2 rise (not depicted) (4, 32, 33)]. Thus, Monsoon Termination II appears to be an event forced by Northern Hemisphere insolation, which follows a number of events not directly forced by Northern Hemisphere insolation.



Although the timing of Monsoon Termination II is consistent with Northern Hemisphere insolation forcing, not all evidence of climate change at about this time is consistent with such a mechanism (Fig. 3). Sea level apparently rose to levels as high as -21 m as early as 135 ky before the present (27, 28), preceding most of the insolation rise. The half-height of marine oxygen isotope Termination II has been dated at 135 ± 2.5 ky (29). Speleothem evidence from the Alps indicates temperatures near present values at 135 ± 1.2 ky (31). The half-height of the δ¹⁸O rise at Devils Hole (142 ± 3 ky) also precedes most of the insolation rise (20). Increases in Antarctic temperature and atmospheric CO₂ (32) at about the time of Termination II appear to have started at times ranging from a few to several millennia before most of the insolation rise (4, 32, 33). On the other hand, Monsoon Termination II coincides within error with the final rise in sea level to full Last Interglacial values (6, 21–23, 28, 34, 35) and the last rise to full Last Interglacial δ¹⁸O at Soreq Cave (12) and Crevice Cave (36). Thus, Monsoon Termination II appears to be an event forced by Northern Hemisphere insolation change, coincident with other such events but after a number of events not directly caused by Northern Hemisphere orbital forcing. As such, it may mark the inception of full interglacial conditions worldwide.

References and Notes

1. W. Dansgaard et al., *Nature* **364**, 218 (1993).
2. The Greenland Summit Ice Cores CD-ROM (1997). Available from the National Snow and Ice Data Center, University of Colorado at Boulder, and the World Data Center-A for Paleoclimatology, National Geophysical Data Center, Boulder, CO. Also available online at www.ngdc.noaa.gov/paleo/icecore/greenland/summit/document/gispisot.htm.
3. Y. J. Wang et al., *Science* **294**, 2345 (2001).
4. W. S. Broecker, G. M. Henderson, *Palaeoceanography* **13**, 352 (1998).
5. Oxygen isotope analyses were performed at the Isotope Laboratory, Institute of Karst Geology, Guilin, China, using a VG MM-903 gas mass spectrometer (for Dongge Cave D3 and D4 analyses, except for D4 between 15.81 ky and 9.98 ky); at the State Key Laboratory of Loess and Quaternary Geology, Institute of Earth Environment, Xi'an, China, using a Finnigan MAT 252 Kiel Device III (Dongge Cave D4 between 15.81 and 9.98 ky); and on a Finnigan MAT 251 at the Nanjing Institute of Geology and Palaeontology, Chinese Academy of Sciences (Hulu Cave H82 between 15.34 and 16.30 ky before the present). Other H82 analyses were reported earlier in (3).
6. R. L. Edwards, J. H. Chen, G. J. Wasserburg, *Earth Planet. Sci. Lett.* **81**, 175 (1987).
7. H. Cheng et al., *Chem. Geol.* **169**, 17 (2000).
8. C.-C. Shen et al., *Chem. Geol.* **185**, 165 (2002).
9. C. H. Hendy, *Geochim. Cosmochim. Acta* **35**, 801 (1971).
10. In detail, D3 and D4 do not replicate perfectly, with some times characterized by differences in δ¹⁸O that are large as compared to analytical error but small compared to the amplitude of the record (Fig. 2). These discrepancies are likely due to kinetic effects, water/rock interactions, and/or differential evaporation of water at the land surface. There is little evidence for kinetic fractionation on the basis of C and O isotope correlations. C and O isotope ratios do not correlate strongly for any of the three stalagmites in this study or even for portions of these

- stalagmites. The highest R² value for any of the three stalagmites is 0.27 (table S6). Because the top of D4 was deposited in isotopic equilibrium and because a portion of D4 replicates the Hulu record, D4 is less likely to have been affected by kinetic effects or water/rock interactions than D3.
11. I. Friedman, J. R. O'Neil, *U.S. Geol. Surv. Prof. Pap.* **440-KK** (1977).
12. M. Bar-Matthews et al., *Geochim. Cosmochim. Acta* **67**, 3181 (2003).
13. D. Fleitmann et al., *Science* **300**, 1737 (2003).
14. R. Gomez, L. Gonzalez, H. Cheng, R. L. Edwards, F. Urbani, *Geol. Soc. Am. Abstr. Programs* **35**, 587 (2003).
15. W. Dansgaard, *Tellus* **16**, 436 (1964).
16. We used the following form of the Rayleigh equation, modified from (37): $(1000 + \delta_p)/(1000 + \delta_{sw}) = f^{(\alpha - 1)}$, where δ_p is the δ¹⁸O of meteoric precipitation, δ_{sw} is the δ¹⁸O of seawater, f is the fraction of the original water vapor remaining, and α is the water/vapor fractionation factor. We assumed a constant α of 1.0094. We used the following values in our calculations: (i) Mid-Holocene/Last Interglacial values: calcite δ¹⁸O_{VPDB} = -9.2‰, temperature 1°C > today, and seawater δ¹⁸O_{SMOW} = 0.0‰. (ii) Today: calcite δ¹⁸O_{VPDB} = -8.1‰ and seawater δ¹⁸O_{SMOW} = 0.0‰. (iii) Glacial times: calcite δ¹⁸O_{VPDB} = -4.5‰ and temperature 4°C. (VPDB, Vienna Pee Dee belemnite standard.)
17. M. A. Maslin, S. J. Burns, *Science* **290**, 2285 (2000).
18. J. Jouzel, G. Hoffmann, R. D. Koster, V. Masson, *Quat. Sci. Rev.* **19**, 363 (2000).
19. C. D. Charles, D. Rind, J. Jouzel, R. D. Koster, R. G. Fairbanks, *Science* **263**, 508 (1994).
20. I. J. Winograd et al., *Quat. Res.* **48**, 141 (1997).
21. J. H. Chen, H. A. Curran, B. White, G. J. Wasserburg, *Geol. Soc. Am. Bull.* **103**, 82 (1991).
22. C. H. Stirling, T. M. Esat, K. Lambeck, M. T. McCulloch, *Earth Planet. Sci. Lett.* **160**, 745 (1998).
23. D. R. Muhs, K. R. Simmons, B. Steinke, *Quat. Sci. Rev.* **21**, 1355 (2002).
24. A. Berger, *J. Atmos. Sci.* **35**, 2362 (1978).

25. J. E. Kutzbach, *Science* **214**, 59 (1981).
26. Z.-S. An, S. Porter, *Geology* **25**, 603 (1995).
27. M. Stein et al., *Geochim. Cosmochim. Acta* **57**, 2541 (1993).
28. C. D. Gallup, H. Cheng, F. W. Taylor, R. L. Edwards, *Science* **295**, 310 (2002).
29. G. Henderson, N. Slowey, *Nature* **404**, 61 (2000).
30. R. G. Fairbanks, *Nature* **342**, 637 (1989).
31. C. Spotl, A. Mangini, N. Frank, R. Eichstadter, S. J. Burns, *Geology* **30**, 815 (2002).
32. J. R. Petit, *Nature* **399**, 429 (1999).
33. M. Bender, T. Sowers, L. Labeyrie, *Global Biogeochem. Cyc.* **8**, 363 (1994).
34. R. L. Edwards, C. D. Gallup, K. B. Cutler, H. Cheng, in *Treatise on Geochemistry, Volume 6: The Oceans and Marine Geochemistry*, H. Elderfield, Ed. (Elsevier, Oxford, 2004), pp. 343–364.
35. N. C. Slowey, G. M. Henderson, V. B. Curry, *Nature* **383**, 242 (1996).
36. J. A. Dorale, thesis, University of Minnesota, Twin Cities, MN (2000).
37. R. E. Criss, *Principles of Stable Isotope Distribution* (Oxford Univ. Press, New York, 1999), p. 108.
38. We especially thank G. Comer and W. S. Broecker for their tremendous and generous support of our work. We thank H. Wang, Y. Fong, and L. Tu for stable isotope analyses and Y. Xie, S. He, J. Cao, Z. Wang, J. Zhan, and D. Yu for assistance with fieldwork. Supported by NSF grants ESH0214041, ESH9809459, and MRI0116395; a Comer Science and Education Foundation Grant (CC8); National Science Foundation of China grants 40328005 and 40231008; and grants from the Ministry of Land and Resources and the Ministry of Science and Technology of China.

Supporting Online Material

www.sciencemag.org/cgi/content/full/304/5670/575/DC1
 Tables S1 to S6
 References

8 September 2003; accepted 24 March 2004

Early Life Recorded in Archean Pillow Lavas

Harald Furnes,^{1*} Neil R. Banerjee,^{1,2†} Karlis Muehlenbachs,² Hubert Staudigel,³ Maarten de Wit⁴

Pillow lava rims from the Mesoarchean Barberton Greenstone Belt in South Africa contain micrometer-scale mineralized tubes that provide evidence of submarine microbial activity during the early history of Earth. The tubes formed during microbial etching of glass along fractures, as seen in pillow lavas from recent oceanic crust. The margins of the tubes contain organic carbon, and many of the pillow rims exhibit isotopically light bulk-rock carbonate δ¹³C values, supporting their biogenic origin. Overlapping metamorphic and magmatic dates from the pillow lavas suggest that microbial life colonized these subaqueous volcanic rocks soon after their eruption almost 3.5 billion years ago.

Biologically mediated corrosion of synthetic glass is a well-known phenomenon (1). Early studies of natural volcanic glass suggested that colonizing microbes can actively dissolve glass substrates to extract nutrients, thereby producing channel-like tubular structures (2, 3). This mechanism has been verified experimentally (4–7). Over the past decade, numerous studies have documented micrometer-sized corrosion structures produced by microbial activity in natural basaltic glasses throughout the upper few hundreds of meters of the oceanic crust (8–13). These

structures have textural characteristics (such as size range, morphology, and organization) that are consistent with a biogenic origin. The presence of carbon and nitrogen (10, 12, 13) as well as nucleic acids associated with the corrosion textures (10, 13) and characteristically depleted δ¹³C values of disseminated carbonate within microbially altered basaltic glass (10, 13, 14) further support the biogenic origin of these structures. In this paper, we document evidence of ancient microbial activity within exceptionally well-preserved pillow lavas of the ~3.5 billion-year-old Bar-

This copy is for your personal, non-commercial use only.

If you wish to distribute this article to others, you can order high-quality copies for your colleagues, clients, or customers by [clicking here](#).

Permission to republish or repurpose articles or portions of articles can be obtained by following the guidelines [here](#).

The following resources related to this article are available online at www.sciencemag.org (this information is current as of November 1, 2015):

Updated information and services, including high-resolution figures, can be found in the online version of this article at:

<http://www.sciencemag.org/content/304/5670/575.full.html>

Supporting Online Material can be found at:

<http://www.sciencemag.org/content/suppl/2004/04/20/304.5670.575.DC1.html>

A list of selected additional articles on the Science Web sites **related to this article** can be found at:

<http://www.sciencemag.org/content/304/5670/575.full.html#related>

This article **cites 29 articles**, 8 of which can be accessed free:

<http://www.sciencemag.org/content/304/5670/575.full.html#ref-list-1>

This article has been **cited by** 211 article(s) on the ISI Web of Science

This article has been **cited by** 38 articles hosted by HighWire Press; see:

<http://www.sciencemag.org/content/304/5670/575.full.html#related-urls>

This article appears in the following **subject collections**:

Atmospheric Science

<http://www.sciencemag.org/cgi/collection/atmos>